Experimental Study of Fe—Mg- and Ca-Distribution Between Coexisting Ortho- and Clinopyroxenes at $P=294$ MPa, $T=750$ and $800°$ C

V.I. Fonarev and A.A. Graphchikov
Institute of Experimental Mineralogy, USSR Acad. Sci., 142432 Chernogolovka, Moscow District USSR

Abstract. The Fe—Mg—Ca-distribution was investigated in synthesis experiments and with the mineral assemblage orthopyroxene + clinopyroxene + quartz. The phase compositions were identified by X-ray diffraction and, where possible, by electron microprobe. The attainment of equilibrium in the run products was signalled by the compositions from control runs (different solutions) becoming closely similar, by recycling runs, by the attainment of equilibrium from different directions (depending on the composition of starting phases), and by special kinetic experiments.

The study produced the following results: (1) the Ca content of the clinopyroxenes decreases with increasing Fe (mol%) from 48.4 at $X_{Cpx}^{Fe}=5$ to 39.8 at $X_{Cpx}^{Fe}=45$ ($800°$ C); from 47.6 at $X_{Cpx}^{Fe}=10$ to 41.7 at $X_{Cpx}^{Fe}=45$ ($750°$ C); increasing temperature expands the stability field of the less calcic clinopyroxenes. (2) The Ca content of orthopyroxenes increases slightly with Fe content from 1.8 at $X_{Opx}^{Fe}=20.5$ to 3.2 at $X_{Opx}^{Fe}=75$; the temperature effect on the Ca content under the T, P conditions of the experiment was not large. (3) Fe and Mg distribution between the coexisting ortho- and clinopyroxenes is largely temperature-dependent, particularly in the compositional range $X_{Opx}^{Fe}=15$–75 mol%; as T increases, Fe redistributes from the rhombic to monoclinic mineral.

Preliminary estimates of rock formation temperatures using the obtained data show that most of the known two-pyroxene geothermometers overstate the actual values by 50–$150°$ C.

Introduction

Orthopyroxenes of the enstatite-ferrosilite and clinopyroxenes of the diopside-hedenbergite solid solution series are common rock-forming minerals which have long attracted scientists as potential indicators of physico-chemical rock forming conditions. Kretz (1963) was the first to infer that temperature affects the Fe—Mg-partitioning between these minerals. Most experimental studies are concerned with enstatite and diopside, Fe-free members of the isomorphous series, while iron-magnesian minerals were only touched upon in the high-temperature, high-pressure region of 810–1,200° C, 15–30 kb ($15 \cdot 10^2$–$30 \cdot 10^2$ MPa) (Lindsley D.H. et al. 1974a,b; Mori 1978; Smith 1972).

Using the experimental evidence available plus mineral thermodynamic characteristics and data on intracrystalline distribution of cations, some authors attempted a two-pyroxene geothermometer on theoretical grounds (Saxena 1976; Wells 1977; Wood and Banno 1973).

Many of the data now available on the compositions of coexisting ortho- and clinopyroxenes require rigorous physicochemical verification. This can only be done on the basis of

experimental evidence which as yet is insufficient, especially for relatively low-temperature and pressure formation conditions of metamorphic rocks.

The present work discusses the results from a study on the Fe—Mg- and Ca-partitioning between coexisting ortho- and clinopyroxenes at 750 and 800° C, 294 MPa.

Experimental Procedure and Technique

Hydrothermal experiments were conducted in a cold-seal high-pressure apparatus with external heating, which is a modification of the Luth and Tuttle design (1963). The design of the electric resistance furnace permitted practically gradient-free ($\pm 3°$ C) zones of 40–50 mm to develop along the pressure vessel axis. The pressures were measured with a Bourdon gauge and maintained to within ± 10 MPa; the temperature measurements with a chromel-alumel thermocouple positioned at analyzed charge level were accurate to $\pm 5°$ C. In the experiments on component distribution among coexisting pyroxenes the oxygen fugacity was controlled with the QFM buffer. The buffer mix in a separate open container was loaded into the pressure vessel; the starting material was pressurized in a gold capsule. Gold capsules were used to prevent losses of iron due to the dissolution in the capsule material. It has been shown (Fonarev et al. 1979; Fonarev and Korolkov 1980; Popp and Frantz 1977) that H_2 – diffusion through the thin Au-wall is fast enough to reach equilibrium between the buffer and the sample in the course of the run. In the NNO-buffered control runs with Fe-rich compositions, the starting pyroxenes decomposed partially to form magnetite. However, no magnetite was detected in the products from the QFM-buffered runs, only to confirm the view that gold capsules are freely permeable to H_2. Experiments were done with both presynthesized pyroxenes and amorphous mixtures. The amorphous mixtures were: A.R. grade chemicals of iron and magnesium oxalates, calcium oxide, and silicon oxide precipitated from ethylorthosilicate. The same reagents were used in the synthesis of starting pyroxenes. Moisture contents were determined for all reagents and accounted for in calculating the bulk compositions of starting mixtures.

Starting Opx[1] with the $X_{Opx}^{Fe}=0$–60[2] and $X_{Opx}^{Ca}=0$ were synthesized at $P=98$ MPa, $T=800°$ C, while those with $X_{Opx}^{Fe}=70$

---

[1] Here and elsewhere in the text: Opx – orthopyroxene; Cpx – clinopyroxene; Q – quartz; Ol – olivine; Amf – amphibole; En – enstatite; Fs ferrosilite; Di diopside; Hd – hedenbergite

[2] For orthopyroxene (X_{Opx}^{Fe}, X_{Opx}^{Ca}) and clinopyroxene (X_{Cpx}^{Fe}, X_{Cpx}^{Ca}),

$$X^{Fe}=\frac{FeO}{FeO+MgO+CaO} \cdot 100 (mol\%),$$
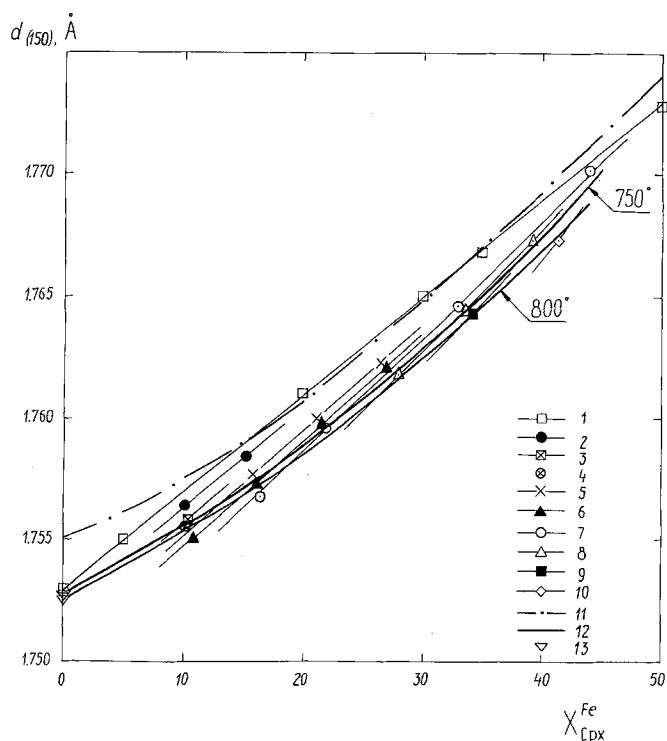
$$X^{Ca}=\frac{CaO}{FeO+MgO+CaO} \cdot 100 (mol\%)$$

Fig. 1. Dependence of the (150) reflection on the Fe- and Ca-contents of clinopyroxenes: $1-10$=isolines are for synthetic clinopyroxenes in which X^{Ca}_{Cpx} (mol%) are $50; 49; 48; 47.5; 47; 46; 45; 44; 43; 41.11$=data of Turnock et al. (1973) for Cpx with $X^{Ca}_{Cpx}=50$ mol%; 12=curves for determining Fe-content of the Cpx coexisting with Opx at $T=750$ and $800°$ C, $P=294$ MPa (see text); 13=Fe-free Cpx synthesized in association with Opx and Ol

point was equal to 20–30 s. Synthetic quartz was used as internal standard. The angular positions of the reflections were calculated from the centre of gravity of the peaks and 2/3 from the base. The Cpx compositions were determined from the (150) reflection. A plot of X^{Fe}_{Cpx} versus $d_{(150)}$ for different Ca-contents in this mineral is presented in Fig. 1. The isolines were drawn for specially synthesized pyroxenes of known compositions with no contaminating phases, at $T=750$ and $800°$ C, $P=294$ MPa, and the oxygen fugacity controlled by the QFM buffer. The duration of the synthesis was 7–10 days. According to Fig. 1, a decrease in the X^{Ca}_{Cpx} is accompanied by a respective decrease in the $d(150)$. Our results agree well with Turnocks et al. (1973) results for $X^{Fe}_{Cpx}=20-40$, but are at variance with their data for more magnesian and Fe-rich compositions. The orthopyroxene compositions were determined from the d-spacing for the (421) and (250) reflections (Fig. 2). The composition – d-spacings relationships for a calcium-free mineral, were established earlier (Fonarev et al. 1980), therefore we have synthesized orthopyroxenes with $X^{Ca}_{Opx}=2$ and 3 mol%, and Fe-content of 40–70 mol%, to determine the effect Ca may have on these reflections. Neither X-ray nor optical examinations of the run products detected any contaminating phases at all. These relations point to an increase in the interplanar spacing of the Opx with decreasing Ca content – this tendency being stronger for (421) than for (250). These two reflections were used to identify the orthopyroxenes in which the Fe-content was less than 60 mol%. In the Fe-richer regions, the (421) reflection was used except in a few cases because the 2θ of the (150) and (250) reflections for clinopyroxene and orthopyroxene, respectively, drew too close together in the X-ray patterns. To avoid the overlapping of reflections in identifying the clinopyroxene compositions from (150), the amount of clinopyroxene in the starting charges for the Fe-rich compositions was twice that of orthopyroxene with the result that the orthopyroxene (250) reflection virtually disappeared from the X-ray patterns of the run products. Special experiments have been carried out to check whether the component partitioning between M1 and M2 sites would affect the reflection positions. The starting materials were the pyroxenes synthesized at $T'=750°$ C (two clinopyroxene samples) and $T=800°$ C (one sample of clinopyroxene and two samples of orthopyroxene) whose relationships are plotted in Figs. 1 and 2. The samples were recycled during 5–7 days at $800°$ C and $750°$ C, respectively, $P-294$ MPa, QFM buffer. The positions of (150) for Cpx, (421) and (250) for Opx were essentially the same as for the starting samples, the difference being within the accuracy of the X-ray analysis ($\theta= \pm 0.01°$). The ferric iron content caused no problem in the mineral composition determinations, owing to very similar T, P and oxygen fugacity conditions in the two sets of experiments – to establish the equilibrium relations and to synthesize compositions for constructing the correlation lines. Also, Mössbauer analyses of some of the samples with $X^{Fe}=5-70$ showed no detectable amounts of Fe^{3+}.

and 80 and $X^{Ca}_{Opx}=0$ – at 490 MPa, $T=800°$ C. Starting clinopyroxenes in which $X^{Fe}_{Cpx}=0-50$, $X^{Ca}_{Cpx}=50$ were synthesized at $P=98$ MPa, $T=650°$ C. The oxygen fugacity was controlled with the QFM buffer in the synthesis of starting orthopyroxenes, and with the MW buffer in the synthesis of starting clinopyroxenes. The duration of synthesis of starting pyroxenes was 7–14 days. X-ray and optical examination of the run products revealed no contaminating phases in the synthesized material. The charges were prepared separately for each run by carefully mixing and grinding the pre-weighed minerals under alcohol in an agate mortar. The weight of the charge in terms of pyroxene, was 36–60 mg, the liquid phase accounting for 30–50 mg. To prevent amphiboles from crystallizing, some of the syntheses were done without introducing water. To keep the partial pressure of water low, some 20 to 200 mg crystalline oxalic acid ($H_2C_2O_4$) were added to the starting charges. All the Fe–Mg–Ca-partitioning runs employed excess (10 to 20 mg) silica which was added either as synthetic quartz or as amorphous silicon oxide (where the synthesis method was used). This proved effective in preventing foreign minerals, say olivine, formation and also in enhancing equilibration rates.

Because of the fine grain-size of the pyroxenes, the phases could rarely be analysed with the electron microprobe. As an alternative, the compositional changes have been monitored by X-ray diffraction methods. X-ray patterns were obtained on a DRON-1 diffractometer with Co-radiation ($CoK_\alpha=1,79021$ Å). The pyroxene compositions were determined by measuring the diffraction peaks from a TUR M62 diffractometer, Co-radiation. The peak profiles were recorded by scanning across the peak at $0.01°$ (θ scale) intervals, the pulse-collection time at every

Experimental Results

Two independent sets of experiments were devised to study the component distribution between the coexisting pyroxenes at $T=750, 800°$ C, and $P=294$ MPa. The first group aimed at evaluating the Ca-saturation in Opx and Cpx, in relation to variations in their Fe contents. These data were then used in the second set of experiments to establish the distribution of all three components between the coexisting minerals over a wide range of compositions. This experimental scheme had to be adopted because of the electron microprobe's limitations. However, these X-ray
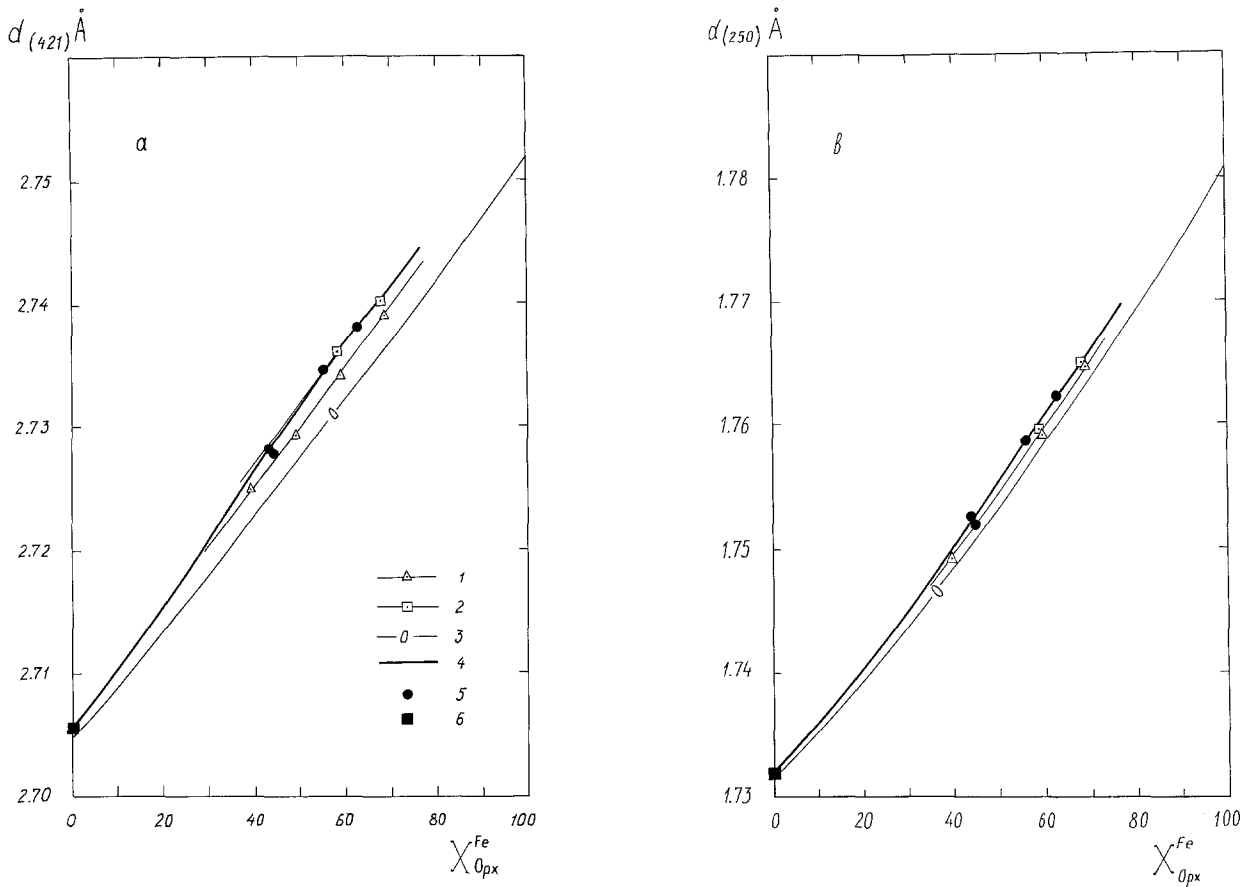
Fig. 2a, b. Dependence of **a** the (421) – and **b** the (250) – reflections on the Fe- and Ca-contents of orthopyroxenes: *1, 2* are for specimens with X_{Opx}^{Ca} 2 and 3 mol% respectively; *3*=data of Fonarev et al. (1980) for Ca-free Opx; *4*=curves for determining the Fe-content in Opx coexisting with Cpx at T=750–800° C, P=294 MPa (see text); *5*=microprobe analyses; *6*=Fe-free orthopyroxenes synthesized in association with Cpx and Ol
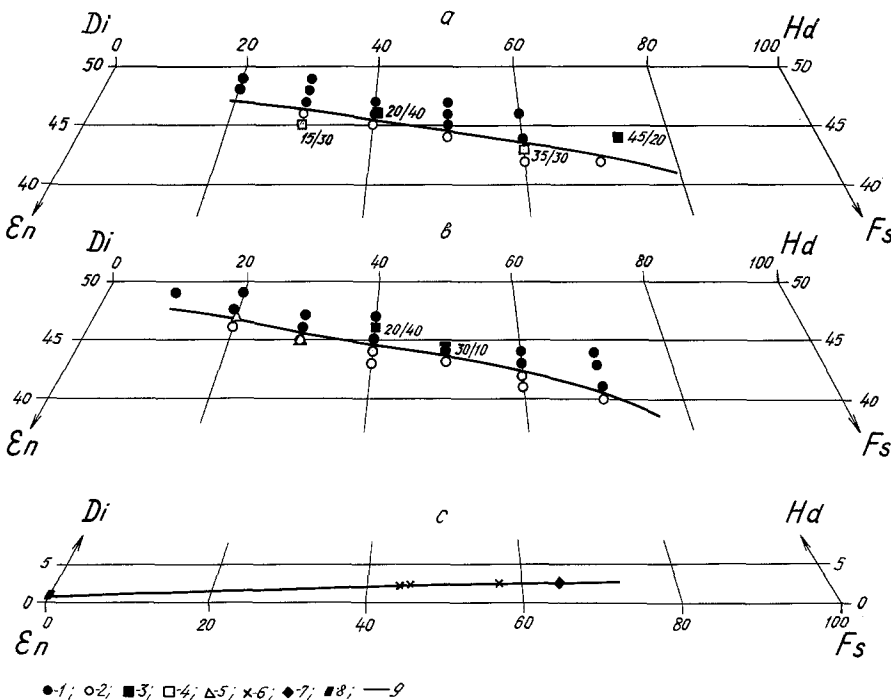

Fig. 3a–c. The Ca-saturation in dependence on the Fe-content at P=294 MPa: **a, b** in clinopyroxenes (assemblage with orthopyroxene) – at 750° C (**a**), 800° C (**b**); **c**=in orthopyroxenes (assemblage with clinopyroxene) – at 750° and 800° C. Runs, performed by the synthesis method: *1*=Opx; *2*=Cpx+Opx. Runs with the mineral assemblage Cpx+Opx (*numbers* indicate the original ratio $X_{Cpx}^{Fe}/X_{Opx}^{Fe}$ with $X_{Cpx}^{Ca}/X_{Opx}^{Ca}$ of 50/0 in all cases): *3*=Cpx; *4*=Cpx+Opx. Runs with synthetic clinopyroxene: *5*=Cpx+Opx. Microprobe analyses of orthopyroxenes: *6*=800° C; *7*=750° C; *8*=Extrapolations of Lindsley and Dixon (1976), Nehru (1976), Warner and Luth (1974); *9*=Opx−Cpx solvus (our data)

Table 1. Compositions of coexisting ortho- and clinopyroxenes as determined in the present study

Run No.	T (°C)	Run duration (days)	Fluid phase	Bulk compositions mol%			Starting materials	Run products				Notes
				$FeSiO_3$	$MgSiO_3$	$CaSiO_3$		Opx		Cpx		
								X^{Fe}	X^{Ca}	X^{Fe}	X^{Ca}	
1	2	3	4	5	6	7	8	9	10	11	12	13
110	800	6	H_2O	13	62	25	amorphous mixture	20.5	1.8	9.3	47.5	tr. Amf.
97	800	8	1 N HCl	17	58	25	$Cpx^*_{25}+Opx^*_{10}+Q$	21.6	1.8	9.0	47.6	
212	800	7	H_2O	15	60	25	$Cpx_{30}+Opx_0+Q$	24.2	2.0	10.4	47.3	
195	800	6	H_2O	23	52	25	$Cpx_{35}+Opx_{10}+Q$	27.6	2.1	12.1	46.7	
211	800	7	H_2O	23	52	25	$Cpx_{25}+Opx_{20}+Q$	29.0	2.1	13.5	46.3	
89	800	11	1 N HCl	30	45	25	$Cpx_{30}+Opx_{30}+Q$	36.5	2.5	17.6	45.4	tr. st. Opx_{30}
337	800	7	2 N HCl	31	44	25	$Cpx_{40}+Opx_{20}+Q$ $+Cpx_{15}+Opx_{50}$	36.5	2.5	17.0	45.6	
90	800	11	1 N NH_4OH	30	45	25	$Cpx_{30}+Opx_{30}+Q$	41.2	2.6	19.6	45.1	
193	800	7	0.25 N HCl	35	40	25	$Cpx_{30}+Opx_{40}+Q$	43.0	2.7	20.6	44.9	
101	800	4	0.25 N HCl	35	40	25	$Cpx_{30}+Opx_{40}+Q$	44.6**	2.62**	24.3	44.3	
101b	800	7	0.25 N HCl	35	40	25	Run 101	43.4**	2.65**	21.3	44.8	
98	800	8	1 N HCl	38	43	19	$Cpx_{35}+Opx_{40}+Q$	44.3**	2.74**	20.6	44.9	
184	800	7	H_2O	35	40	25	amorphous mixture	46.0	2.7	22.0	44.7	
107	800	4	0.25 N HCl	40	35	25	$Cpx_{40}+Opx_{40}+Q$	49.3	2.8	24.1	44.4	
108	800	4	H_2O	40	35	25	$Cpx_{40}+Opx_{40}+Q$	50.2	2.8	24.8	44.3	
154	800	6	0.25 N HCl	45	30	25	$Cpx_{40}+Opx_{50}+Q$	55.25**	2.9**	30.6	43.3	
154b	800	2	0.25 N HCl	45	30	25	$Cpx_{40}+Opx_{50}+Q$	56.8	3.0	27.3	43.8	st. Cpx_{40} and Opx_{50}
154c	800	10	0.25 N HCl	45	30	25	$Cpx_{40}+Opx_{50}+Q$	56.8	3.0	30.4	43.3	
177	800	17	H_2O	48	27	25	$Cpx_{35}+Opx_{60}+Q$	62.0	3.1	34.3	42.7	tr. st. Cpx_{35}
354	800	9	1 N HCl	49	20	31	$Cpx_{50}+Opx_{40}$ $+Cpx_{35}+Opx_{80}+Q$	63.5	3.1	35.8	42.3	
364	800	9	H_2O	48	23	29	$Cpx_{35}+Ol_{60}$ $+Ol_{70}+Q$	65.0	3.1	37.6	41.9	
280	800	9	H_2O	53	14	33	$Cpx_{50}+Opx_{60}+Q$	72.0	3.2	44.4	39.9	Ol_{91}
280b	800	10	H_2O	53	14	33	Run 280	70.5	3.2	43.0	40.4	
155	800	14	H_2O	60	15	25	$Cpx_{50}+Opx_{70}+Q$	68.0	3.2	45.4	39.8	Ol_{88} and st. Opx_{70}
155b	800	8	H_2O	60	15	25	Run 155	72.9	3.2	44.4	39.9	Ol_{90} and tr. st. Opx_{70}
368	750	8	–	24	49	27	$Cpx_{40}+Opx_{10}$ $+Cpx_{10}+Opx_{40}$ $+Q+H_2C_2O_4$	35.8	2.4	16.7	46.2	
237a	750	9	H_2O	25	50	25	$Cpx_{30}+Opx_{20}+Q$	36.5	2.5	16.2	46.3	Amf
292	750	8	H_2O	32	35	33	$Cpx_{30}+Opx_{30}+Q$	44.5	2.7	19.6	45.7	
349	750	8	H_2O	35	40	25	Run 327$+Cpx_{30}$ $+Opx_{40}+Q$ $+H_2C_2O_4$	47.0	2.8	20.2	45.6	
293	750	7	0.25 N HCl	35	40	25	$Cpx_{30}+Opx_{40}+Q$	48.8	2.8	22.3	45.3	
293a	750	9	H_2O	35	40	25	Run 293	48.8	2.8	21.3	45.4	
327	750	10	solution***	35	40	25	$Cpx_{30}+Opx_{40}+Q$	50.1	2.8	22.3	45.3	
279a	750	3	H_2O	37	38	25	$Cpx_{30}+Opx_{40}+Q$	52.6	2.9	24.4	45.1	st. Cpx_{35} and Opx_{40}
279b	750	8	H_2O	37	38	25	$Cpx_{35}+Opx_{40}+Q$	50.2	2.8	22.1	45.3	
279c	750	12	H_2O	37	38	25	$Cpx_{35}+Opx_{40}+Q$	51.0	2.9	23.4	45.2	
351	750	9	1 N HCl	39	30	31	$Cpx_{40}+Opx_{30}$ $+Cpx_{20}+Opx_{70}+Q$	52.5	2.9	24.4	45.0	
322	750	10	solution***	43	27	30	$Cpx_{45}+Opx_{40}+Q$	58.5	3.0	24.0 and 29.0	45.1 and 44.4	
322a	750	10	H_2O	43	27	30	Run 322	59.0	3.0	26.8	44.7	
228a	750	7	H_2O	50	25	25	$Cpx_{50}+Opx_{50}+Q$ $+H_2C_2O_4$	62.5**	3.01**	31.0	44.2	
370	750	8	1 N HCl	44	25	31	$Cpx_{40}+Opx_{60}+Q$ $+Opx_{60}+Cpx_{30}$	62.2	3.1	29.5	44.3	
310	750	10	H_2O	47	21	32	$Cpx_{45}+Opx_{50}+Q$	66.0	3.1	34.1	43.7	
311	750	10	H_2O	50	20	30	$Cpx_{50}+Opx_{50}+Q$	67.0	3.1	35.9	43.4	
295	750	10	H_2O	48	21	31	$Cpx_{40}+Opx_{60}+Q$	not determined		40.0	42.7	
295a	750	7	H_2O	48	21	31	Run 295	68.5	3.2	37.0	43.3	

Table 1 (continued)

Run No.	T (°C)	Run duration (days)	Fluid phase	Bulk compositions mol%			Starting materials	Run products				Notes
								Opx		Cpx		
				FeSiO$_3$	MgSiO$_3$	CaSiO$_3$		X^{Fe}	X^{Ca}	X^{Fe}	X^{Ca}	
1	2	3	4	5	6	7	8	9	10	11	12	13
315	750	6	H$_2$O	51	18	31	Cpx$_{45}$+Opx$_{60}$+Q	69.2	3.2	37.4	43.2	
350	750	6	1 N HCl	51	18	31	Cpx$_{50}$+Opx$_{50}$+Q +Opx$_{80}$+Cpx$_{30}$	69.5	3.2	37.3	43.2	
326	750	10	H$_2$O	54	15	31	Cpx$_{50}$+Opx$_{60}$+Q	72.8 and 64.0	3.2 and 3.1	41.3	42.5	
326a	750	5	H$_2$O	54	15	31	Run 326	72.5	3.2	41.3	42.5	
329	750	8	2 N NH$_4$OH	54	15	31	Cpx$_{50}$+Opx$_{60}$+Q +H$_2$C$_2$O$_4$	73.7	3.2	43.2	42.1	
371	750	9	H$_2$O	57	12	31	Cpx$_{50}$+Opx$_{70}$+Q	75.1	3.2	45.2	41.7	Ol$_{90}$

* The numbers correspond to X_{Cpx}^{Fe} and X_{Opx}^{Fe}; in all starting pyroxenes $X_{Opx}^{Ca}=0$ and $X_{Cpx}^{Ca}=50$

** Orthopyroxene compositions determined by the electron microprobe

*** Fe, Mg and Ca dissolved in HCl

Notes: 1. Bulk compositions contain additional 15–50 wt.% SiO$_2$

2. Run products from all runs contain quartz

3. Fe content in olivine determined by X-ray difraction (Fonarev et al. 1979)

4. tr. st. – trace starting

relationships (Figs. 1 and 2) only can be used where the Ca-content of the coexisting minerals is known.

The Ca-saturation in clinopyroxenes associated with orthopyroxenes was mainly determined by the synthesis method; the results were verified in a number of runs by the mineral assemblage method (Fig. 3a, b). In the first method, the boundaries of one-phase (Cpx)[3] and two-phase (Cpx+Opx) fields of the synthesis area were defined by varying the bulk compositions of the starting mix with respect to the Ca and Fe contents.

The appearance of Opx was checked by optical and X-ray methods. A rather strong peak (420) proved effective in identifying as low as 1.5–2 wt.% orthopyroxene in the charge, which makes the X_{Cpx}^{Ca} determination accurate to 0.6–1 mol%. In the mineral assemblage method the boundary between the single- and two-phase fields was defined either by the complete disappearance of the known Opx from the starting mixture Cpx+Opx, or by the appearance of Opx upon decomposition of the crystalline Cpx. While most runs were performed with pure H$_2$O, those in which the bulk Fe content (mol%) was 5.1 (800° C), 10.2 and 10.4 (750° C), used crystalline oxalic acid (H$_2$C$_2$O$_4$). Run duration, normally, was 7 or occasionally 10 (for crystalline phases) days at 800° C and 10 days at 750° C.

As is shown in Fig. 3, the experimental results at each temperature are fairly consistent, and what is more, runs with crystalline phases lend full support to the results from the synthesis experiments. So it is evident that the Ca-content of the mineral decreases with increasing Fe, to confirm earlier findings (Lindsley et al. 1974a,b; Mori 1978).

Increasing temperatures expand the stability fields of less calcic clinopyroxenes associated with orthopyroxenes – this effect is much stronger with Fe-rich members of the solid solution series, and only negligible in magnesian-bearing solutions. The

Ca-saturation in orthopyroxene associated with clinopyroxene were determined by the electron microprobe ("Camebax") in the run products from four runs (101b, 98, 228a, 154[4]; Table 1). The orthopyroxene prismatic grains in the products from these runs are up to 30 µm across. At least five orthopyroxene grains were analyzed from each run using an accelerating potential of 15 kV and a sample current of $4 \cdot 10^{-7}$–$10 \cdot 10^{-7}$ A. Natural pyroxenes of the known composition and oxides of the analyzed elements were used as standards. The results were refined on a computer; the program contained corrections for the atomic number, absorption and fluorescence of the elements. The maximum error of the analysis was within ± 1.5–2% relative.

The results showed a very good agreement (Fig. 3c). Furthermore, no temperature-dependent differences in the Ca-content of the orthopyroxenes have been detected within the analytical accuracy and this agrees with earlier studies (Lindsley and Dixon 1976; Lindsley et al. 1974a,b; Mori 1978; Mori and Green 1976; Nehru 1976; Werner and Luth 1974), which showed that temperature variations by 50° resulted in 0.5 mol% changes in the Ca content in Opx. We found (Fig. 3) that the Ca-content in orthopyroxenes increases slightly with increasing Fe in the mineral. Extrapolations into the Fe-free area for $P=294$ MPa agreed with the results obtained by several authors (Lindsley and Dixon 1976; Mori and Green 1976; Warner and Luth 1974). From the data available on the Ca-saturation in clino- and orthopyroxenes, X-ray relationships can be established to determine the equilibrium Fe/Fe+Mg+Ca ratio in coexisting pyroxenes. The respective working lines are given in Figs. 1 and 2. They were constructed by projecting the Ca-saturation values on the isolines for Ca-contents in the minerals within the d(h k l) versus X^{Fe} coordinates for 750 and 800° C, respectively. The orthopyroxene compositions were used as given by the microprobe analysis for runs 101b, 98, 228a, 154. Note that these curves are only to be used for determining the equilibrium pyroxene composi-

---

3 Runs were performed with excess (1–3 mg) silica. Therefore, here we have, strictly speaking, a two-phase (Cpx+Q) and a three-phase (Cpx+Opx+Q) region

4 Analysis by Prof. C.E. Nehru, New-York University, USA

tions and only at $T=750$, $800°$ C, $P=294$ MPa, i.e. for the composition of clinopyroxene in association with orthopyroxene (Fig. 1) and vice versa (Fig. 2).

The relations (determinative curves) shown in Figs. 1 and 2 can be expressed through the following equations for $T=800°$ C:

$$X_{Cpx}^{Fe} = -171719.885 + 192383.3212\,d_{(150)} - 53864.6409\,d_{(150)}^2 \quad (1)$$

$$X_{Opx}^{Fe} = 28107.1544 - 22561.2599\,d_{(421)} + 4499.1187\,d_{(421)}^2 \quad (2)$$

$$X_{Opx}^{Fe} = -22534.9533 + 23770.8414\,d_{(250)} - 6212.3454\,d_{(250)}^2 \quad (3)$$

and for $T=750°$ C:

$$X_{Cpx}^{Fe} = -181331.26 + 203329.128\,d_{(150)} - 56981.263\,d_{(150)}^2 \quad (4)$$

Inasmuch as the Ca-contents in Opx for 750 and 800° C are the same, we used (2) and (3) to find X_{Opx}^{Fe} at 750° C. The second set of experiments which aimed at determining the compositions of coexisting ortho- and clinopyroxenes was performed with a mineral assemblage (the mineral assemblage method), and a few synthesis experiments (Table 1). The accuracy of the results was the primary concern. Replicate X-ray measurements gave the maximum error of not greater than $\pm 0.01°$ (θ scale). The compositions of the coexisting minerals were determined only from the run products for which the profiles of the pyroxene diffraction peaks afforded measurements within the accuracy of the X-ray analysis. Analysis of the possible experimental (Figs. 1–3) and X-raying errors gave the average accuracy of the phase composition determinations ± 0.5, ± 1 mol% for the Ca-content and ± 1.5–2, ± 1–1.5 mol% for the Fe-content in the ortho- and clinopyroxene, respectively. Independent measurements of the orthopyroxene compositions in the run products from the two reflections were largely consistent within the stated limits.

To determine the optimal equilibration time, two series of kinetic experiments were done at 800 and 750° C, with 0.25 N HCl and bidistilled H_2O solutions, respectively. The results
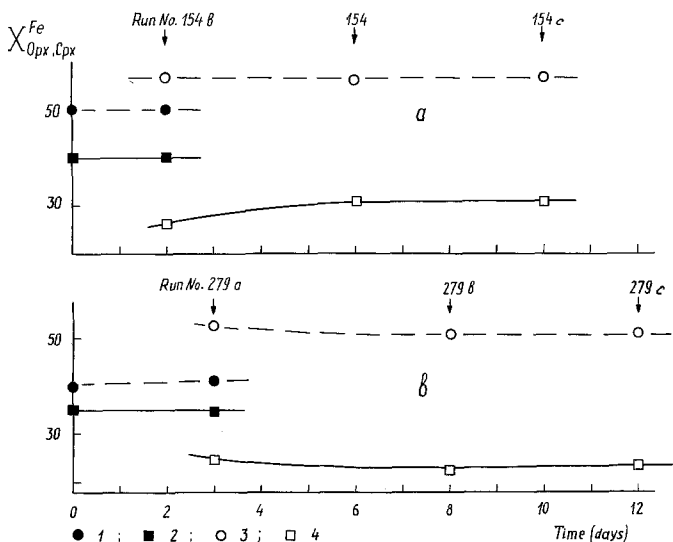

Fig. 4a, b. Results of the kinetic experiments to determine equilibria in the assemblage Opx + Cpx + Q, a $T=800°$ C and b 750° C. Starting minerals: $1=$ Opx; $2=$ Cpx. Newly-formed minerals: $3=$ Opx; $4=$ Cpx
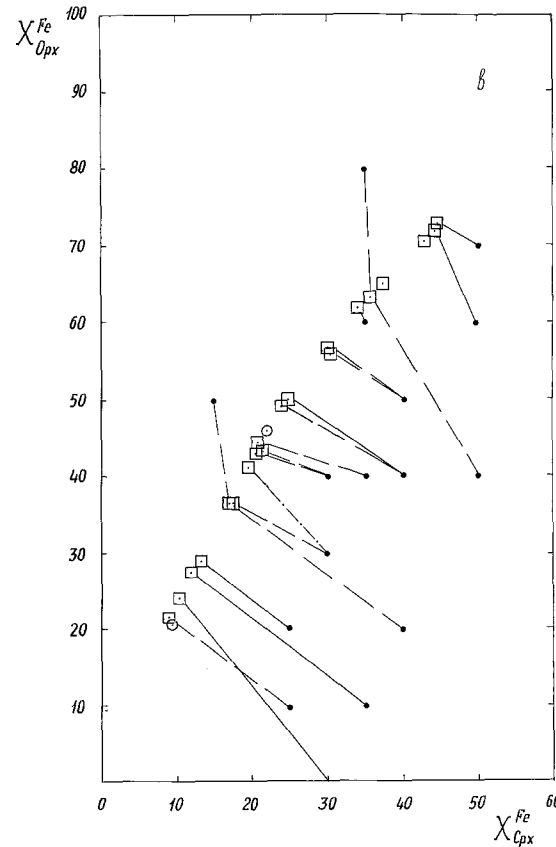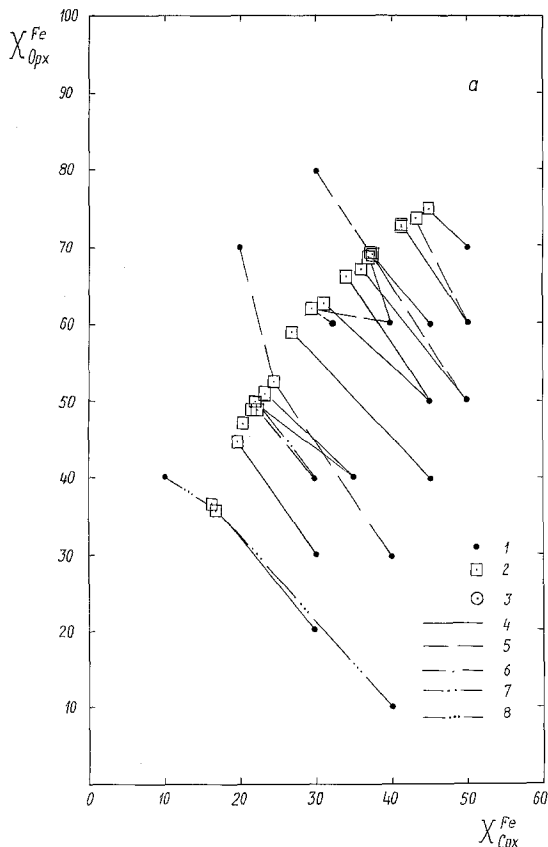

Fig. 5a, b. Experimental data on the compositions of coexisting ortho- and clinopyroxenes at $P=294$ MPa a at $T=750°$ C and b at 800° C: $1=$ Fe content in the starting pyroxenes; $2=$ runs with mineral assemblage; $3=$ runs by the synthesis method. The fluid composition: $4=H_2O$; $5-$ HCl solution; $6=NH_4OH_{solution}$; $7=$ Fe, Mg and Ca dissolved in HCl; $8=H_2C_2O_4\cdot 2H_2O$
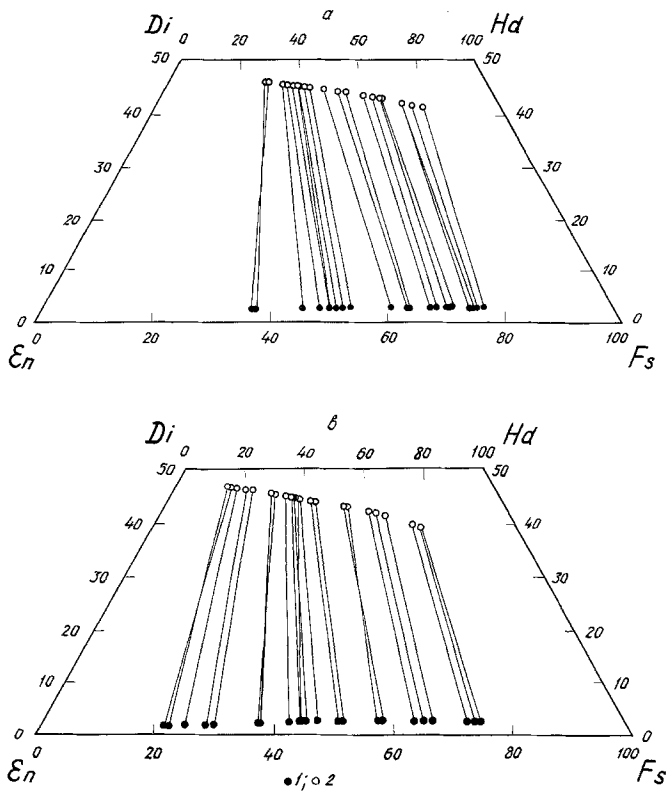
Fig. 6a, b. The pyroxene quadrilateral showing experimental data on the compositions of coexisting pyroxenes at $P=294$ MPa **a** at $T=750°$ C and **b** at $800°$ C: $1=$Opx; $2=$Cpx

(Table 1, Fig. 4) from the two series were practically identical and agreed well with earlier studies of the reactions that involved minerals of varying compositions (Fonarev et al. 1978, 1979). The minerals decomposed at the earliest reaction stages, with the newly-formed phases undergoing rapid crystallisation. It is characteristic that while even in long runs the new minerals retained their composition the starting phases usually disappeared completely within the first 2–3 days of the run. All these data clearly indicate that the newly-formed ortho- and clinopyroxenes are of equilibrium compositions and that, in the general case, it will take minerals four days to reach equilibrium. Table 1, Figs. 5 and 6 present the experimental results on the component partitioning between the coexisting ortho- and clinopyroxenes. For each run, the Ca content of the minerals can be determined from the diagrams in Fig. 3. To provide a check on the data and to confirm the attainment of equilibrium, various means were used: recycling certain runs, varying run duration, liquid phase composition and proportions by weight of the starting phases. Some of the experiments were performed in two stages: the quenched specimen was carefully ground, X-rayed and the run was resumed under the same $T-P$ conditions (Runs 293, 293a, 326, 326a). In other runs, the synthesis method (110, 184) was used. According to Table 1 and Fig. 5, the results for each isotherm (750 and 800° C) are grouped closely despite the very different experimental conditions, so that the points fitted smoothly onto the isotherms. Although occasionally this tendency was affected by certain kinetic factors, recycling the runs helped in attaining equilibrium (runs 101b, 155b, 322a, 295a). In none of the cases did electron microprobe analyses of the pyroxenes (Table 1) reveal grains of different composition, or zoning within a single grain. For example, in each of the 5

grains analysed from run 228a, the composition was determined three times (in the centre and margins). Normally, estimates varied by as much as 0.2 mol% for Fe-content and 0.1 mol% for Ca, with only one exception of 0.7 and 0.3 mol%, respectively. In other runs, the greatest measured differences for individual grains were not higher than 1–1.3 mol% for Fe and 0.2–0.4 mol% for Ca. Both shape and intensity of ortho- and clinopyroxene diffraction peaks confirm that the run products do not contain minerals which vary by more than 1–1.5 mol% in composition excepting the presence of the remains of the starting pyroxenes.

It must be noted, however, that the above results were obtained for charges in which clinopyroxenes were more Fe-rich, and orthopyroxenes more Mg-rich than equilibrium compositions would normally be (Fig. 5). All our attempts with phase compositions taken in inverse proportions produced no noticeable results – the run products revealed starting minerals alone, irrespective of run duration. It was only when experimental charges contained two clinopyroxenes and two orthopyroxenes of different composition that the reaction continued to the end and equilibrium was achieved (runs 337, 354, 368, 351, 370, 350). This must be connected with certain kinetic peculiarities of the reactions involved but further experiment will be required to clear up the matter. Runs with compositions richest in Mg (110, 237a) and Fe (155b, 280, 371), produced amphiboles (of the tremolite-actinolite series) and olivines, respectively. The results from these runs point out the fields with divariant assemblages Opx+Cpx+Amf+Q and Opx+Cpx+Ol+Q though their exact boundaries still have to be defined.

Discussion and Conclusion

As a result of this study, the Fe—Mg- and Ca-partitioning between coexisting pyroxenes was established experimentally. The ratios of all isomorphous components in the minerals were found to have changed considerably over the 750–800° C range. As the temperature increases, iron redistributes from the rhombic into the monoclinic mineral; decreasing the Ca-content in the clinopyroxene. The temperature dependence of the redistribution is very distinct for the compositional range 15–75 mol% (for Opx), declining somewhat toward Mg- and Fe-richer regions. The present paper is too short to make a detailed comparison between our results and the mineral-formation temperatures from the known two-pyroxene geothermometers. We would need to evaluate the effects the pressure and various additional components present in natural pyroxenes will have on the two-pyroxene equilibrium. However, a preliminary comparison can already be done at this stage. Figure 7 presents the compositions of the coexisting minerals for which the temperatures of formation were determined using Wood and Banno (Bohlen and Essene 1979; Jayawardena and Carswell 1976), and Saxena (1976) geothermometers. For charnockites and pyroxene-granulites from Sri-Lanka, Jayawardena and Carswell (1976) found $858\pm11°$ C from Wood and Banno-geothermometer, and $700\pm50°$ C from a garnet-clinopyroxene equilibrium which agrees with our findings of about 700° C.

The mineral formation temperatures for pyroxene-bearing metamorphic rocks from the Adirondacks as estimated with a two-pyroxene geothermometer were 711–850° C (Bohlen and Essene 1979), with an average of 790° C (from 23 analyses). Here again, our data (Fig. 7) point to lower temperatures, apparently not higher than 650–700° C.

Saxena (1976) in using his two-pyroxene geothermometer placed the formation temperatures for some charnockites in the
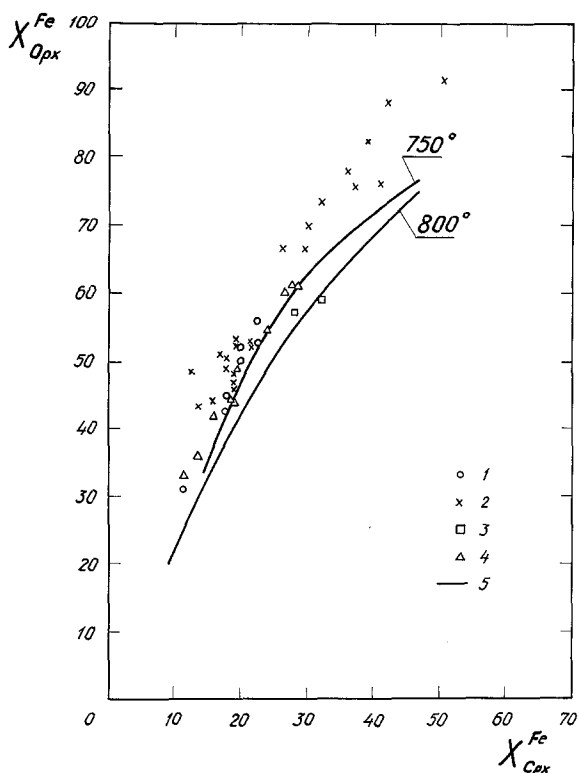
Fig. 7. Compositions of coexisting pyroxenes in several granulites and charnockites. *1* = Jayawardena and Carswell (1976): $T = 858 \pm 11°$ C; *2* = Bohlen and Essene (1979): $T = 711-850°$ C; *3* = Saxena (1976): $T = 700-725°$ C; *4* = Saxena (1976): $T = 760-870°$ C; *5* = the present data for $T = 750$ and $800°$ C

700–870° C range. However, there appears to be a reverse temperature dependence of the component redistribution when these data are compared with our findings – the mineral compositions with crystallisation temperatures of 700–725° C (Saxena) plot close to our 800° C-isotherm, while, as we have found, specimens with formation temperatures 760–870° C cannot exist above 750° C. Application of Wells' (1977) and Perchuk's (1970) geothermometers also indicated crystallisation temperatures that were too high as compared with the above experimental data. It is noteworthy that although the above comparison does not aim at evaluating precise temperatures, it nonetheless clearly shows the necessity for refining the two-pyroxene geothermometers now available, expecially in the region of moderate and lower temperatures. It is believed that the experimental results from this study combined with published data (for a higher-temperature region) could form, given the appropriate thermodynamic treatment, the basis for constructing a geothermometer which would assess reliably the actual mineral-forming processes.

References

Bohlen SR, Essene EJ (1979) A critical evaluation of two-pyxene thermometry in Adirondack granulites. Lithos 12:335–345

Fonarev VI, Dokina TN, Korolkov GJa (1980) Synthesis and unit-cell parameters for orthopyroxenes of the enstatite-ferrosilite series. Zapiski Vsesojuznogo mineralogicheskogo obschestva, No 2:243–246

Fonarev VI, Korolkov GJa (1980) The assemblage orthopyroxene + cummingtonite + quartz. The low-temperature stability limit. Contrib Mineral Petrol 73:413–420

Fonarev VI, Korolkov GJa, Dokina TN (1976) Experimental study of the stability of the assemblage rhombic pyroxene + magnetite + quartz under hydrothermal conditions. Geokcimiya 10:1498–1511

Fonarev VI, Korolkov GJa, Dokina TN (1979) Stability fields in the assemblage cummingtonite-olivine-quartz from experimental evidence. Geokhimiya 7:984–996

Jayawardena DEDe S, Carswell DA (1976) The geochemistry of "charnockites" and their constituent ferromagnesian minerals from the Precambrian of south-east Sri-Lanka (Ceylon). Mineral Mag 40:541–554

Kretz R (1963) Distribution of magnesium and iron between orthopyroxene and calcic pyroxene in natural mineral assemblages. J Geol 71:773–785

Lindsley DH, Dixon SS (1976) Diopside-enstatite equilibria at 850–1400° C, 5–35 kbar. Am J Sci 276:1285–1301

Lindsley DH, King HEJr, Turnock AC, Grover JE (1974a) Compositions of synthetic augite and hypersthene co-existing at 810° C: application to pyroxenes from lunar highlands rocks. Geophys Res Lett 1:134–136

Lindsley DH, King HEJr, Turnock AC, Grover JE (1974b) Phase relations in the pyroxene quadrilateral at 980° C and 15 kbar. Geol Soc Am, Abstr Progr 6:846

Luth WC, Tuttle OF (1963) Externally heated cold-seal pressure vessels for use to 10,000 bars and 750° C. Am Mineral 48:1401–1403

Mori T (1978) Experimental study of pyroxene equilibria in the system $CaO - MgO - FeO - SiO_2$. J Petrol 19:45–65

Mori T, Green DH (1976) Subsolidus equilibria between pyroxenes in the $CaO - MgO - SiO_2$ system at high pressures and temperatures. Am Mineral 61:616–625

Nehru CE (1976) Pressure dependence of the enstatite-diopside solvus. Am Mineral 61:578–581

Perchuk LL (1970) Equilibria of rockforming minerals. Nauka, Moscow

Popp RK, Frantz JD (1977) Diffusion of hydrogen in gold. Annu Rept Dir Geophys Lab Carnegie Inst, 1976–1977. Washington, DC, pp 662–664

Saxena SK (1976) Two-pyroxene geothermometer: a model with an approximate solution. Am Mineral 61:643–652

Smith D (1972) Stability of iron-rich pyroxene in the system $CaSiO_3 - FeSiO_3 - MgSiO_3$. Am Mineral 57:1413–1428

Turnock AC, Lindsley DH, Grover JE (1973) Synthesis and unit cell parameters of $Ca - Fe - Mg$ pyroxenes. Am Mineral 58:50–59

Warner RD, Luth WC (1974) The diopside-orthoenstatite two phase region in the system $CaMgSi_2O_6 - Mg_2Si_2O_6$. Am Mineral 59:98–109

Wells PRA (1977) Pyroxene thermometry in simple and complex systems. Contrib Mineral Petrol 62:129–139

Wood BJ, Banno S (1973) Garnet-orthopyroxene and orthopyroxene-clinopyroxene relationships in simple and complex systems. Contrib Mineral Petrol 42:109–124